Microwave-assisted arbitrary optical-pulse generation in a thermal vapor

Rajitha K. V.* and Tarak N. Dey†
Indian Institute of Technology Guwahati, Guwahati-781 039, Assam, India
(Received 18 May 2016; published 28 November 2016)

The propagation of a weak optical field through an atomic system in closed Λ configuration is investigated in which the hyperfine levels are coupled by a microwave pulse. Under the three-photon resonance condition, it is observed that a new pulse of the shape of a microwave field is generated at the probe transition while the input probe is absorbed. The generated probe pulse follows the temporal position of the microwave pulse and maintains shape through the propagation. A simple propagation equation for the probe field in the Fourier domain has been employed to study this effect. This shape preservation of the probe pulse is due to the ground state coherence of the hyperfine transitions induced by the weaker intensity of the microwave field. The generation of an arbitrary shaped probe pulse is also possible at comparable strength of control and microwave fields. The intensity and detuning of the microwave field can play an important role to control probe pulse properties such as gain, broadening, and preservation of shape. The mechanism of efficient generation and manipulation of an optical pulse may have important applications in information science and optical communications.

DOI: 10.1103/PhysRevA.94.053851

I. INTRODUCTION

Quantum coherence effects in three-level atomic media has been a topic of great interest for many years [1] because it leads to many counterintuitive phenomena. Of particular interest is the phenomenon of electromagnetically induced transparency (EIT) and related effects due to their ability to drastically modify the optical properties of the medium [2–6]. EIT leads to a plethora of new applications such as slow light [7], stored light [8], and stopped light [9], which are based on controlled two-photon processes. Optical systems modeled in three-level atomic configurations can be generalized by introducing more levels and couplings between different levels with optical and low-frequency microwave fields [10,11]. These systems are shown to exhibit many new properties. Some of the interesting observations include four-wave mixing of optical and microwave fields [12,13], study of double dark resonances [14,15], etc. A low-frequency field coupling two lower levels (LLs) along with two optical fields form a closed three-level Λ system [16–21]. In closed Λ systems, the LL field perturbs the EIT and induces new coherences which lead to better control over optical properties of the media such as dispersion, absorption, and nonlinearity [16–24]. Studies in closed Λ systems make use of perturbed low-frequency coherence induced by the additional field resulting in better storage and retrieval of light [24], changing light propagation [25], phase manipulation of EIT [17], and generation of new frequencies [19,26]. It is observed that the coherent dynamics of a Λ system is enhanced due to interference between two- and three-photon processes when an additional field is applied, which couples the ground state to an additional metastable state [27]. In this work, we exhibit how an optical pulse is generated at one transition frequency of a Λ system which has the shape of a microwave pulse coupling the lower levels, when a control field couples the other transition. This generation occurs by a suitable choice of detunings so that three-photon processes get enhanced, while two-photon EIT effects are completely suppressed. Under three-photon resonance, the shape, detuning, and intensity of microwave field can be used for optical-pulse generation with controllable width and gain.

II. THEORETICAL MODEL

In this paper, we exploit microwave induced hyperfine coherence to generate efficient generation of the optical frequency pulse. In order to demonstrate efficient frequency conversion, we use an inhomogeneously broadened closed Λ atomic system consisting of an excited state $|1\rangle$ and two metastable states $|2\rangle$ and $|3\rangle$ as shown in Fig. 1. The electric dipole allowed transitions $|1\rangle \leftrightarrow |3\rangle$ and $|1\rangle \leftrightarrow |2\rangle$ are coupled by two optical fields, namely, probe and control fields, whereas the magnetic dipole allowed transition $|2\rangle \leftrightarrow |3\rangle$ is coupled by a microwave field to form a closed Λ system. This level structure can be experimentally realized in ^{87}Rb which contains ground levels $|2\rangle = |5S_{1/2}, F = 2, m = 2\rangle$ and $|3\rangle = |5S_{1/2}, F = 1, m = 0\rangle$ and the excited level $|1\rangle = |5P_{3/2}, F' = 2, m = 1\rangle$. Numerical studies of the Maxwell-Bloch (MB) equation enable us to understand the coherent control of the optical frequency generation and subsequent propagation through an inhomogeneously broadened system. The system is shown to exhibit interesting behavior under the condition when amplitudes and detunings of the microwave and two other optical fields are properly selected. The generated pulse is amplified and follows the temporal profile of microwave pulse. To interpret these results, we derive a simple expression for the atomic coherence at probe transmission in the Fourier domain. From this, we conclude that the generation of an arbitrary shaped optical pulse is a direct manifestation of perturbed hyperfine coherence by microwave field.

The structure of the three coupling fields is given by

$$\vec{E}_i(z,t) = \hat{e}_i \mathcal{E}_i(z,t) e^{-i(\omega_i t - k_i z + \phi_i)} + \text{c.c.} \qquad (i \in p,c,\mu), \tag{1}$$

*rajitha@iitg.ac.in
†tarak.dey@iitg.ernet.in

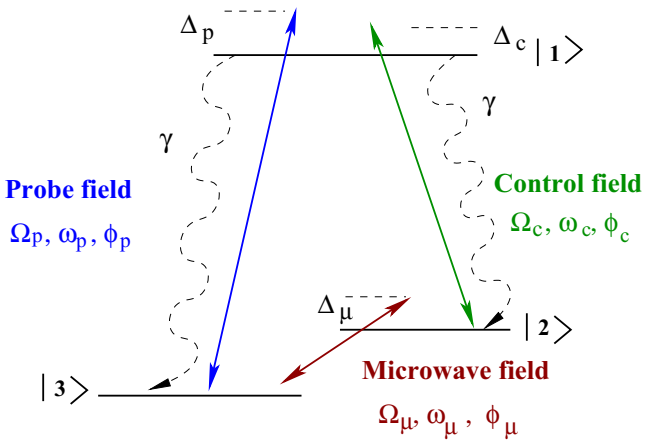

FIG. 1. Schematic representation of three-level atoms in closed Λ configuration. The control field $\boldsymbol{E}_c$ couples to the transition $|1\rangle \leftrightarrow |2\rangle$, the probe field $\boldsymbol{E}_p$ interacts with the transition $|1\rangle \rightarrow |3\rangle$, and the microwave pulse $\boldsymbol{E}_\mu$ couples the hyperfine levels $|3\rangle \rightarrow |2\rangle$. For simplicity, we consider $\gamma_1 = \gamma_2 = \gamma/2$.

where $\mathcal{E}_i$ is the space-time-dependent amplitude, ω_i the frequency, and ϕ_i the phase of the corresponding fields. The Hamiltonian of the system under dipole and rotating wave approximations can be expressed as

$$\begin{aligned} H_{\rm int} &= \hbar\omega_{13}\,|1\rangle\langle 1| + \hbar\omega_{12}\,|2\rangle\langle 2| \\ &\quad - \hbar\Omega_c e^{-i(\omega_c t - k_c z + \phi_c)}\,|1\rangle\langle 2| \\ &\quad - \hbar\Omega_p e^{-i(\omega_p t - k_p z + \phi_p)}\,|1\rangle\langle 3| \\ &\quad - \hbar\Omega_\mu e^{-i(\omega_\mu t - k_\mu z + \phi_\mu)}\,|2\rangle\langle 3| + \text{H.c.}, \end{aligned} \tag{2}$$

where the Rabi frequencies of the probe, control, and microwave fields are defined by

$$\begin{aligned} &\Omega_p = \vec{\boldsymbol{d}}_{13}\cdot\vec{\mathcal{E}}_p/\hbar, \quad \Omega_c = \vec{\boldsymbol{d}}_{12}\cdot\vec{\mathcal{E}}_c/\hbar, \\ &\Omega_\mu = \vec{\boldsymbol{\mu}}_{23}\cdot\vec{\mathcal{E}}_\mu/\hbar, \end{aligned} \tag{3}$$

respectively. The electric and magnetic dipole matrix elements are represented by $\vec{\boldsymbol{d}}_{ij}$ and $\vec{\boldsymbol{\mu}}_{ij}$, respectively. Now we introduce a unitary transformation to the wave function of the system so that explicit time dependence is eliminated from the interaction terms of the Hamiltonian. The transformation operator U takes the form

$$U = e^{-i\{(\omega_p t - k_c z + \phi_c)|1\rangle\langle 1| - [(\omega_p+\omega_c)t - (k_p+k_c)z + (\phi_p+\phi_c)]|2\rangle\langle 2|\}}. \tag{4}$$

With the unitary transformation, the effective interaction Hamiltonian takes the form

$$\begin{aligned} H_{\rm int} &= -\hbar\Delta_p\,|1\rangle\langle 1| - \hbar(\Delta_p - \Delta_c)\,|2\rangle\langle 2| - [|1\rangle\langle 3|\,\Omega_p \\ &\quad + |1\rangle\langle 2|\,\Omega_c + |2\rangle\langle 3|\,\Omega_\mu e^{-i(\Delta t + \Delta k z + \Phi)} + \text{H.c.}]. \end{aligned} \tag{5}$$

The relative phase and wave vector mismatch are defined as $\Phi = \phi_p - \phi_c - \phi_\mu$, and $\Delta k = k_p - k_c - k_\mu$ with k_i being the propagation constant of the respective field. The detunings of the three fields from the corresponding transition resonance are given by

$$\Delta_p = \omega_p - \omega_{13}, \quad \Delta_c = \omega_c - \omega_{12}, \quad \Delta_\mu = \omega_\mu - \omega_{23}, \tag{6}$$

respectively. The three-photon detuning Δ is defined as $\Delta = \Delta_p - \Delta_c - \Delta_\mu$.

Now we impose the condition on the field frequencies $\omega_p = \omega_c + \omega_\mu$, which gives $\Delta = 0$, so that the time dependence is completely eliminated from the Hamiltonian. Note that the two-photon resonance condition of electromagnetically induced transparency case, $\omega_p - \omega_c = \omega_{23}$, modifies into condition $\omega_p - \omega_c = \omega_{23} + \Delta_\mu$, satisfied by the three detunings, in the presence of an additional coupling field between hyperfine levels. This condition not only simplifies the numerical integration but also turned out to be important for effective frequency generation.

The spatiotemporal propagation of probe and control fields is governed by Maxwell's equations in the slowly varying envelope approximation as

$$\left(\frac{\partial}{\partial z} + \frac{1}{c}\frac{\partial}{\partial t}\right)\Omega_p = i\eta_p\rho_{13}, \tag{7}$$

$$\left(\frac{\partial}{\partial z} + \frac{1}{c}\frac{\partial}{\partial t}\right)\Omega_c = i\eta_c\rho_{12}, \tag{8}$$

where the coupling constant is defined as $\eta_i = \gamma\mathcal{N}\lambda_i^2/8\pi$ $(i \in p,c)$. Typical parameter values are $\mathcal{N} = 5\times10^{11}$ atoms/cm^3, $\lambda_p = 780$ nm, and $\gamma = 2\pi\times10^6$ Hz. Note that the ratio $\eta_\mu/\eta_p = (\omega_m/\omega_p)\alpha^2$, where $\alpha \approx 1/137$ is the fine-structure constant. It follows that $\eta_\mu \ll \eta_p, \eta_c$. Therefore the spatiotemporal effects of the microwave field are not taken into account in the numerical integration of Maxwell's equations since the absorption is much smaller than optical fields. The quantum dynamics of the atoms is modeled by the master equation approach. The dynamics of atomic coherences that governs the propagation of probe field are given by Bloch equations

$$\begin{aligned} \dot\rho_{11} &= -2\gamma\rho_{11} + i\Omega_c^*\rho_{21} - i\Omega_c^*\rho_{12} + i\Omega_p\rho_{31} - i\Omega_p^*\rho_{13}, \\ \dot\rho_{12} &= -[\gamma - i\Delta_c]\rho_{12} - i\Omega_c(\rho_{11} - \rho_{22}) \\ &\quad + i\Omega_p\rho_{32} - i\Omega_\mu^* e^{i\theta}\rho_{13}, \\ \dot\rho_{13} &= -[\gamma - i\Delta_p]\rho_{13} + i\Omega_c\rho_{23} \\ &\quad - i\Omega_p(\rho_{11} - \rho_{33}) - i\Omega_\mu e^{-i\theta}\rho_{12}, \\ \dot\rho_{22} &= \gamma\rho_{11} - i\Omega_c\rho_{21} + i\Omega_c^*\rho_{12} + i\Omega_\mu e^{-i\theta}\rho_{32} - i\Omega_\mu^* e^{i\theta}\rho_{23}, \\ \dot\rho_{23} &= -[\Gamma - i(\Delta_p - \Delta_c)]\rho_{23} + i\Omega_c^*\rho_{13} \\ &\quad - i\Omega_p\rho_{21} + i\Omega_\mu e^{-i\theta}(\rho_{33} - \rho_{22}), \end{aligned} \tag{9}$$

where $\theta = \Phi + \Delta k z$. The spontaneous decay of excited state $|1\rangle$ to metastable states is denoted by γ, whereas Γ is the decay rate of the hyperfine coherence. The atoms in the hot gas medium at room temperature are in random motion and have a velocity associated with each. The Doppler shift in frequency caused by the finite velocity of the atoms is taken into account in our simulation by averaging the coherences over the Maxwell-Boltzmann velocity distribution of the moving atoms.

$$\langle\rho_{ij}\rangle = \frac{1}{\sqrt{\pi w_D^2}}\int_{-\infty}^{\infty}\rho_{ij}(kv)e^{-(kv/w_D)^2}d(kv). \tag{10}$$

The Doppler width w_D at temperature T is defined by $\sqrt{2k_BTv_p^2/\mathcal{M}c^2}$ where $\mathcal{M}$ is the atomic mass and k_B the Boltzmann constant. We have included velocity induced Doppler shift by replacing detunings Δ_i to $\Delta_i(v) = \Delta_i - k_i v (i \in p,c)$ in Eq. (9). We investigated the spatiotemporal evolution of the fields by numerically solving the coupled full MB equations. The control field can be on-resonance or off-resonance with the transition $|1\rangle \leftrightarrow |2\rangle$. The probe and microwave fields are detuned accordingly from resonance to fulfill the three-photon resonance condition as stated earlier. The propagation equations (7) and (8) are solved in a rotating frame moving with the velocity of light in vacuum c; $\tau = t - z/c$, $\zeta = z$. With this choice of variables, the partial differential equations can be modified to ordinary differential equations as

$$\frac{d\Omega_p}{d\zeta} = i\eta_p\langle\rho_{13}\rangle, \tag{11}$$

$$\frac{d\Omega_c}{d\zeta} = i\eta_c\langle\rho_{12}\rangle, \tag{12}$$

where the angular brackets denote Doppler averaging.

III. NUMERICAL RESULTS

We investigate the spatiotemporal evaluation of probe field in the presence of a constant control field and an arbitrary shaped microwave pulse. We chose the temporal profile of the microwave field as a multiple peaked Gaussian or a secant-hyperbolic envelope. The time-dependent envelope for both microwave and probe fields can be written as

$$\Omega_j(\zeta = 0,\tau) = \Omega_j^0 \sum_i f_{j_i} H\left[\frac{\tau - \tau_{j_i}}{\sigma_{j_i}}\right] \qquad (j \in p,\mu), \tag{13}$$

$$H[x] = e^{-x^{2\alpha_{j_i}}} \quad \text{Gaussian profile,} \tag{14}$$

$$H[x] = \text{sech}(x) \quad \text{secant-hyperbolic profile,} \tag{15}$$

where Ω_j^0, σ_{j_i}, and f_{j_i} are the amplitude, temporal width, and strength of the individual envelope, respectively. The parameter α_{j_i} gives the flatness of an individual envelope peak. The desired pulse shape can be obtained by using spatial light modulators [28]. The initial amplitudes of the three fields are taken as $\Omega_c^0 = 1.41\gamma$, $\Omega_p^0 = 0.1\gamma$, and $\Omega_\mu^0 = 0.07\gamma$. Thus both probe and microwave field intensities are considerably smaller than the control field intensity. Figure 2(a) shows the temporal variation of probe and microwave pulse at different propagation distances. The shape of the probe field at medium boundary $\zeta = 0$ is chosen as a cw, whereas the microwave field profile is double Gaussian. It can be seen that the shape of the microwave pulse has been generated in the probe profile. The initial cw probe field is fully suppressed and a pulse with the shape of the double Gaussian pulse is generated towards the exit of the medium. It is noticeable that the temporal profile of the pulse once formed, propagates unaltered throughout the medium. In Fig. 2(b) the hyperfine coherence is plotted in the presence and absence of the microwave field. We notice in Fig. 2(b) that the hyperfine coherence is negligible in the absence of the microwave field, whereas the microwave field substantially modifies the hyperfine coherences. The

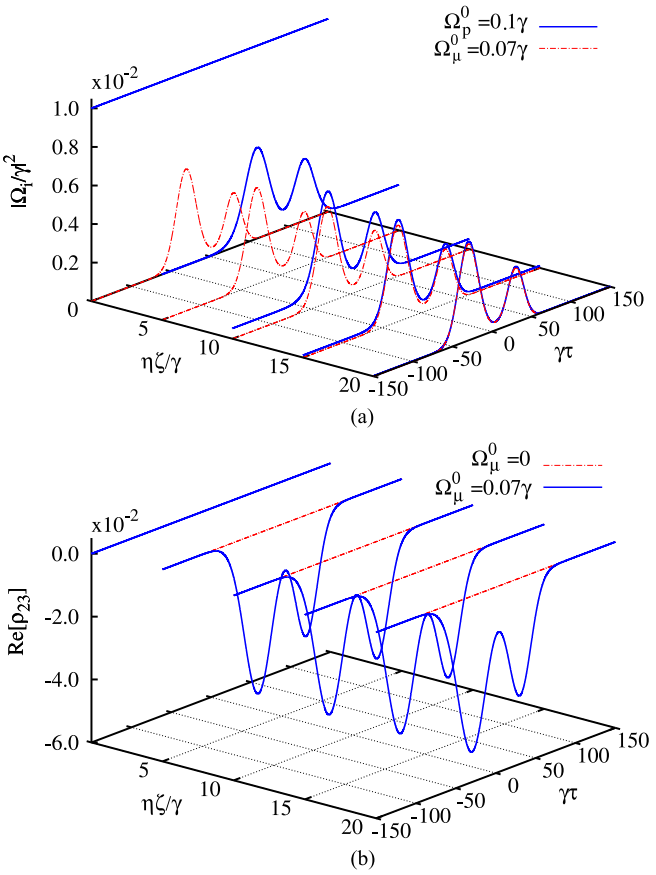

FIG. 2. (a) Temporal profiles of probe and microwave fields are plotted at different propagation distances $\eta\zeta/\gamma$ of the medium. Initial envelopes of probe and microwave fields are taken to be as cw and multipeak Gaussian structure, respectively. (b) The spatiotemporal evolution of hyperfine coherence ρ_{23} is plotted in the presence and absence of a microwave field. The width, strength, and location of individual peaks for the microwave envelope are $\sigma_{\mu_1} = 25/\gamma$, $\sigma_{\mu_2} = 20/\gamma$, $f_{\mu_1} = 1$, $f_{\mu_2} = 0.75$, $\tau_{\mu_1} = -30/\gamma$, $\tau_{\mu_2} = 30/\gamma$, respectively. The following parameters have been used to generate these plots: $\Omega_c^0 = 1.41\gamma$, $\Delta_p = 2\gamma$, $\Delta_c = 0.6\gamma$, $\Delta_\mu = 1.4\gamma$, $w_D = 50\gamma$, $\Delta k/k = 1.8 \times 10^{-5}$, and $\Phi = 0$.

profile of induced coherence is identical to the shape of the microwave field. Hence the distinct characteristic of atomic coherence changes by the microwave field leads to the observed phenomena.

Next we examine the relative intensity dependence on the propagation dynamics of the probe field by taking microwave intensity of comparable strength as the control field intensity. We take the initial shape of the probe pulse as super-Gaussian, whereas the microwave pulse is a multipeak secant-hyperbolic one. As can be seen from Fig. 3(a), the probe shape is replaced by the microwave profile and propagates as a shape preserving pulse. The broadening and distortion of the probe pulse at propagation length $\eta\zeta/\gamma = 100$ in the presence and absence of the microwave field is shown in Fig. 3(b). This figure confirms unambiguously that the width of the generated probe pulse broadens due to the strong intensity of the microwave field, whereas weak microwave pulse intensity generates a probe pulse with a width the same as the input microwave shape. We

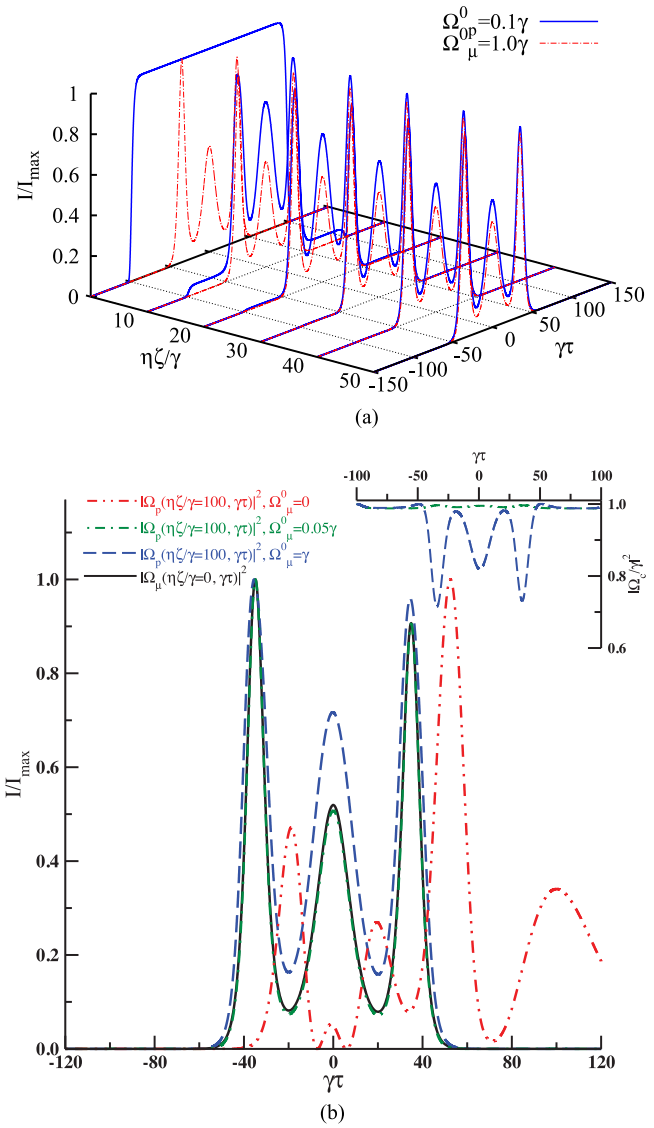

FIG. 3. (a) Normalized intensity of a weak probe (solid blue line) and a strong multipeaked secant-hyperbolic microwave (dot-dashed red line) pulse are plotted along the length of the inhomogeneously broadened medium. (b) Normalized probe pulse intensity $I/I_{\max}$ at the medium exit at $\eta\zeta/\gamma = 100$ for different intensities of microwave field. The initial profile of the microwave is shown by a solid black line. To facilitate the analysis of the pulse broadening and distortion, all pulses are shown normalized to their respective peak values. The parameters are the same as in Fig. 2 except $\Omega_c = \gamma$, $\Delta_c = 0$, $\Delta_p = \Delta_\mu = 2\gamma$, $\sigma_{p_1} = 50/\gamma$, $\tau_p = 0$, $\sigma_{\mu_1} = \sigma_{\mu_3} = 5/\gamma$, $\sigma_{\mu_2} = 10/\gamma\,\tau_{\mu_1} = -\tau_{\mu_3} = 5/\gamma$, $\tau_{\mu_2} = 0$, and $\alpha_{p_1} = 20$.

also find that the integrated transmission of the generated probe profile for strong and weak microwave field cases are about 280% and 1%, respectively. Therefore the transmission and width of the generated probe pulse can be efficiently controlled by suitably choosing the intensity of the microwave field. Figure 3(b) also exhibits how the conventional EIT system fails to protect the propagation of an arbitrary shaped probe pulse propagating through thermal medium. For this purpose, we consider that the time-dependent envelope of input probe pulse is the same as shown in Fig. 3(b) by a black solid line with

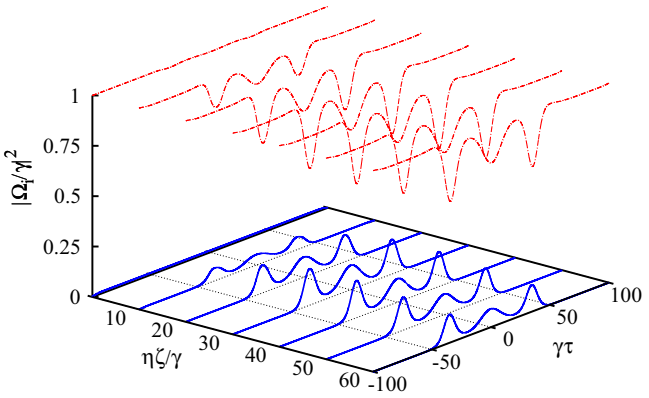

FIG. 4. The temporal evolution of the probe (solid blue line, $i = p$) and control (dot-dashed red line, $i = c$) fields are plotted at different propagation distances $\eta\zeta/\gamma$ of the medium in the presence of a multipeak secant-hyperbolic shaped microwave field. The parameters are the same as in Fig. 3(a).

$\Omega^0_p = 0.1\gamma$. It is evident from the red double-dotted-dashed line in Fig. 3(b) that the temporal profile of the probe field is completely distorted during propagation due to the presence of higher order dispersion although the transmission is about 20%. Hence the stringent condition for distortionless pulse propagation is that the width of the transparency window created by the control field should be sufficiently larger than the the spectral width of the probe pulse. Otherwise the arbitrary probe pulse suffers from distortion and absorption. It is also evident from the inset of Fig. 3(b) that the control field has a shape which is an inversion of microwave field shape in the strong regime. On the other hand, the change in the control field shape is very negligible at weak microwave fields. The inverted shape of the multipeak secant-hyperbolic structure in the control field profile also explains how the generated probe field acquires a gain from the control field as depicted in Fig. 4. This figure also shows how the noninverted and inverted multipeak secant-hyperbolic structures in the generated probe field as well as in the control field propagate through the medium with unaltered shape [29,30]. This suggests that the dynamical evolution of the control field becomes important in the strong regime.

The effect exhibited by the system is independent of the input shapes of probe and microwave fields. To verify this, we further studied the propagation dynamics of the probe field with different shapes of microwave fields. In all cases, it has been observed that the probe pulse is absorbed and got replaced by the microwave pulse shape and it follows the temporal location and dynamics of the microwave pulse.

From these results it is evident that the initial probe field has no significant role in the subsequent dynamics of the generated pulse. The initial pulse is totally absorbed by the medium and a new pulse at the same frequency is generated with the shape of the microwave pulse. This fact is demonstrated by Fig. 5 where the probe pulse dynamics is shown without any input probe coupling. As the input probe is absent, we have taken $\Delta_p = 0$, and the other two detunings values are $\Delta_c = 1.4\gamma$ and $\Delta_\mu = 0.6\gamma$. As can be seen, a pulse is generated at the probe frequency which was initially absent. The generated pulse is

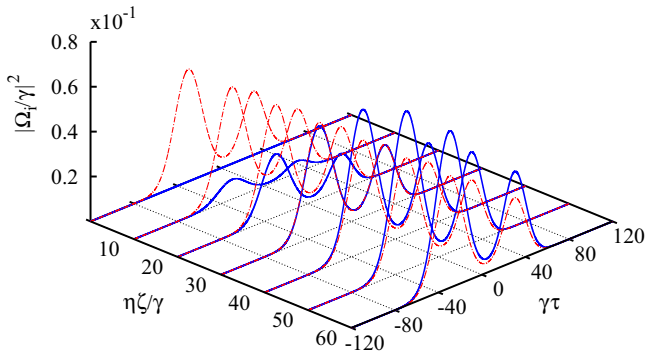

FIG. 5. Probe (solid blue line, $i = p$) and microwave (dot-dashed red line, $i = \mu$) pulse intensities are plotted as a function of time at different propagation distances $\eta\zeta/\gamma$ of the medium without input probe. The parameters are the same as in Fig. 2 except that the intensity and detuning of the input probe are zero. The probe intensity is increased by 2.5 times for the sake of clarity of the figure.

amplified. From the comparison with Fig. 2, it is clear that the pulse is generated at a larger propagation distance in the absence of input probe coupling. So the input probe coupling field has no direct influence on the pulse dynamics, but it enhances the generation at smaller distances and subsequently gets absorbed by the medium.

Finally we study how the arbitrary shaped optical-pulse generation of a closed Λ system is strongly dependent on two- and three-photon processes in the presence of a weak probe field. Figure 6 depicts the temporal behavior of the generated optical pulse at a length of $\eta\zeta/\gamma = 40$. The normalized intensity profile of input microwave pulse is shown by the black solid line in Fig. 6. It is observed from Fig. 6 that the generated optical pulse develops oscillatory distorted behavior by considering two particular conditions: (i) all three fields are in resonance condition ($\Delta_c = \Delta_p = \Delta_\mu = 0$) and (ii) when control and probe fields fulfill two-photon resonance condition ($\Delta_p - \Delta_c = 0$), whereas the microwave field is on resonance $\Delta_\mu = 0$. It is clearly shown in Fig. 6 that the efficient optical-pulse generation is possible when the three-photon resonance condition is satisfied, i.e., $\Delta_p - \Delta_c - \Delta_\mu = 0$ and $\Delta_\mu \neq 0$. From this it is clear that the condition of three-photon resonance where two-photon resonance breaks down is crucial in observing efficient frequency generation and undistorted propagation. The detunings of the three fields can take any reasonable values as long as three-photon resonance is satisfied. Hence the microwave pulse not only generates an optical pulse with its own shape but also protects the probe pulse which can now propagate without distortion through the medium. This is not possible otherwise, in a conventional EIT system.

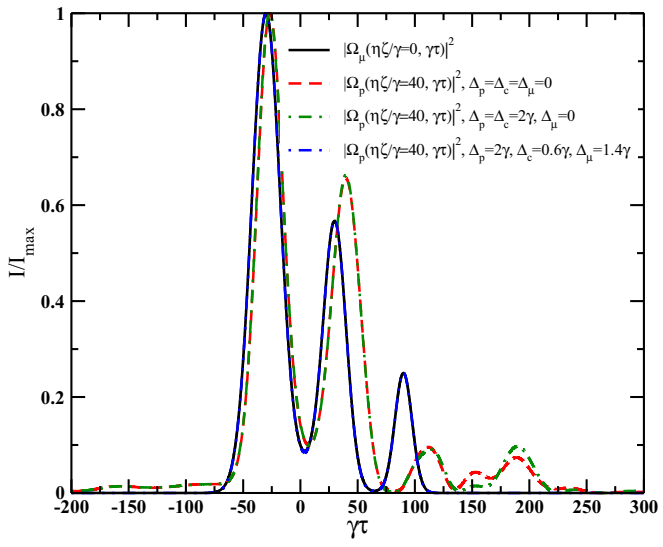

FIG. 6. The normalized intensities of generated optical pulses are plotted as a function of time at a length $\eta\zeta/\gamma = 40$ of the medium in the presence of a weak microwave field. The parameters are the same as in Fig. 2 except for the initial microwave profile. The initial profile of the microwave is shown by a solid black line. The width, strength, and location of individual peaks for the microwave envelope are $\sigma_{\mu_1} = 25/\gamma$, $\sigma_{\mu_2} = 20/\gamma$, $\sigma_{\mu_3} = 15/\gamma$, $f_{\mu_1} = 1$, $f_{\mu_2} = 0.75$, $f_{\mu_3} = 0.5$, $\tau_{\mu_1} = -30/\gamma$, $\tau_{\mu_2} = 30/\gamma$, and $\tau_{\mu_3} = 90/\gamma$, respectively.

IV. ANALYSIS AND DISCUSSIONS

In order to analyze the results, we assume that the probe and microwave fields are sufficiently weak ($\Omega_c \gg \Omega_p \gg \Omega_\mu$) so that we can pursue the perturbative approach. In the limit of weak probe and much weaker microwave fields, the ground state population $\rho_{33} \approx 1$. We considered terms of first order in the probe and microwave fields and all orders in the control field. Therefore the full Bloch equations can be approximated as

$$\dot{\rho}_{13} = -[\gamma - i\Delta_p]\rho_{13} + i\Omega_c\rho_{23} + i\Omega_p,$$
$$\dot{\rho}_{23} = -[\Gamma - i(\Delta_p - \Delta_c)]\rho_{23} + i\Omega_c^*\rho_{13} + i\Omega_\mu e^{i\theta}. \quad (16)$$

We decompose the Rabi frequency Ω_j, $(j \in p,\mu)$ and density matrix ρ_{ij} into its Fourier components

$$\Omega_j(\zeta,\tau) = \int_{-\infty}^{\infty} e^{-i\omega\tau}\tilde{\Omega}_j(\zeta,\omega)d\omega \ \ (j \in p,\mu), \quad (17)$$
$$\rho_{ij}(\zeta,\tau) = \int_{-\infty}^{\infty} e^{-i\omega\tau}\tilde{\rho}_{ij}(\zeta,\omega)d\omega\,. \quad (18)$$

From Eqs. (16), we obtain

$$\tilde{\rho}_{13}(\zeta,\omega) = \frac{i\Gamma_{23}\tilde{\Omega}_p - e^{i\theta}\Omega_c^0\tilde{\Omega}_\mu}{\Gamma_{13}\Gamma_{23} + |\Omega_c^0|^2}, \quad (19)$$

where the relaxation rates are defined by $\Gamma_{13} = \gamma + i\Delta_p - i\omega$, $\Gamma_{23} = \Gamma + i(\Delta_c - \Delta_p) - i\omega$. The propagation of the probe [Eq. (8)] takes the following form in the Fourier domain:

$$\frac{\partial\tilde{\Omega}_p}{\partial\zeta} = i\eta_p\langle\tilde{\rho}_{13}\rangle. \quad (20)$$

Using Eq. (19),

$$\frac{\partial\tilde{\Omega}_p}{\partial\zeta} = i\eta_p\left\langle\frac{i\Gamma_{23}\tilde{\Omega}_p}{\Gamma_{13}\Gamma_{23} + |\Omega_c^0|^2} - \frac{e^{i\theta}\Omega_c^0\tilde{\Omega}_\mu}{\Gamma_{13}\Gamma_{23} + |\Omega_c^0|^2}\right\rangle. \quad (21)$$

The angular bracket denotes averaging over the inhomogeneous broadening for the detunings. The above equation (21) gives an insight into the pulse generation. The first term

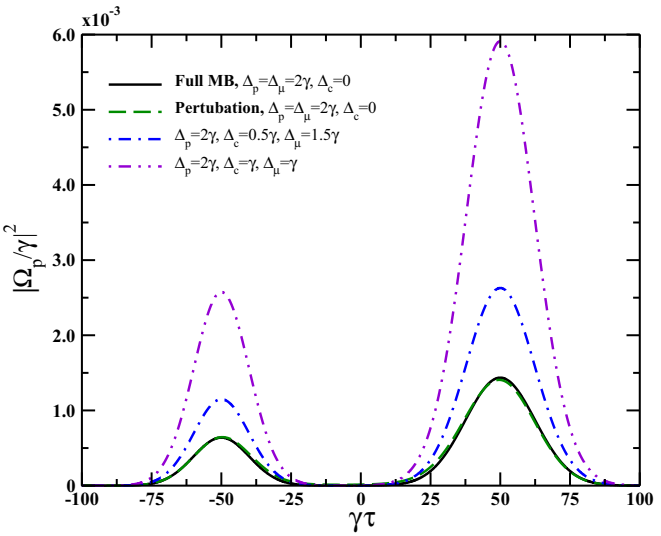

FIG. 7. Transmission of the weak probe field at a distance $\eta\zeta/\gamma = 100$ in the presence of a double Gaussian shaped microwave field. The parameters are same as in Fig. 2 except $\sigma_{\mu_1} = 20/\gamma$, $\sigma_{\mu_2} = 25/\gamma$.

within the angular brackets refers to the EIT phenomenon which renders opaque medium transparent for the probe field under the two-photon resonance condition. The second term corresponds to a gain process involving the microwave field at off-resonance condition. Therefore competition between these two terms governs the spatiotemporal evolution of the probe. The key to the optical frequency generation mechanism is three-photon resonance in which the two-photon condition simultaneously breaks down. Hence the first term suppresses the initial probe envelope due to the presence of medium absorption at single-photon probe detuning, whereas the second term generates a pulse with microwave envelope shape. Note that we considered a constant control field. The dynamics also depend on the total phase through the second term. This gives better controllability on the probe dynamics. Furthermore, Eq. (21) is similar to Eq. (16) of Li *et al.* [17], wherein the controllable transmission of the probe field was achieved by using a cw microwave field, whereas in the present investigation an arbitrary microwave pulse leads to the generation of a shape preserving probe pulse in a medium consisting of a closed lambda system.

Equation (21) is to be integrated in order to compare the perturbative results with full MB equations. We assume the initial profile of the microwave field is a double peak structure, while the control and probe fields are cw and Gaussian shape, respectively. The results shown in Fig. 7 exhibit how the results obtained from perturbation theory are in full agreement with the results of full MB equations. In Fig. 7, we have also shown that the transmission of the generated probe pulse can be varied by choosing different control and microwave field detunings. The integrated transmission intensity of the output probe pulse is about 1% for $\Delta_p = 2\gamma$, $\Delta_\mu = 2\gamma$, $\Delta_c = 0$, whereas $\Delta_p = 2\gamma$, $\Delta_\mu = \gamma$, $\Delta_c = \gamma$ gives rise to 38% probe intensity transmission. Hence the choice of detuning of the microwave field plays an important role in controlling transmission of the generated pulse. The generated pulse travels with the velocity of light. These equations clearly show that the result is a manifestation of competition between two- and three-photon processes. For the selected parameters, the three-photon process dominates over the two-photon process, which exhibits EIT, and the optical pulse is generated and amplified. It is evident from Eq. (21) that it is not necessary to have an input probe pulse for the observed phenomena.

V. CONCLUSION

In this paper, we have shown a scheme for generation of optical pulse of arbitrary shapes in a three-level Λ atomic medium exploiting the microwave induced atomic coherence between hyperfine levels. The optical pulse generated at the probe transition frequency follows the temporal profile of the input microwave pulse connecting the hyperfine levels of the atomic system. It is also demonstrated that the input probe pulse has only a transient effect in the generated pulse dynamics. The generated probe pulse with an arbitrary shape propagates throughout the length of the medium, which is not possible in a conventional EIT system. The phenomenon is shown to be a result of competition between two- and three-photon resonances where three-photon resonance dominates over the two-photon resonance. The numerical results also show that the generation and shape preserving dynamics of probe pulses are possible at comparable strength of control and microwave fields. The intensity and detuning of the microwave field play an important role in controlling the gain and broadening of the generated probe. With this scheme an optical pulse of desired shape can be efficiently generated and controlled. This may be exploited in precision measurements where stable optical frequency is preferred over microwave frequency.

ACKNOWLEDGMENT

R.K.V. and T.N.D. are grateful to DST FIST programme at Physics Department, IIT Guwahati for high computational facility (Grant No. SR/FST/PSII-0202/2009).

[1] E. Arimondo, Prog. Opt. **35**, 257 (1996).
[2] M. O. Scully and M. S. Zubairy, *Quantum Optics* (Cambridge University Press, Cambridge, 1997).
[3] S. E. Harris, Phys. Today **50**, 36 (1997).
[4] S. E. Harris, Phys. Rev. Lett. **70**, 552 (1993).
[5] M. Fleischhauer, A. Imamoglu, and J. P. Marangos, Rev. Mod. Phys. **77**, 633 (2005).
[6] O. Kocharovskaya and Y. I. Khanin, Sov. Phys. JETP **63**, 945 (1998).
[7] L. V. Hau, S. E. Harris, Z. Dutton, and C. H. Behroozi, Nature (London) **397**, 594 (1999).
[8] D. F. Phillips, A. Fleischhauer, A. Mair, R. L. Walsworth, and M. D. Lukin, Phys. Rev. Lett. **86**, 783 (2001).

[9] O. Kocharovskaya, Y. Rostovtsev, and M. O. Scully, Phys. Rev. Lett. **86**, 628 (2001).
[10] M. S. Shahriar and P. R. Hemmer, Phys. Rev. Lett. **65**, 1865 (1990).
[11] D. V. Kosachiov, B. G. Matisov, and Y. V. Rozhdestvensky, J. Phys. B **25**, 2473 (1992).
[12] A. S. Zibrov, A. B. Matsko, and M. O. Scully, Phys. Rev. Lett. **89**, 103601 (2002).
[13] A. S. Zibrov, A. A. Zhukov, V. P. Yakovlev, and V. L. Velichansky, JETP Lett. **83**, 136 (2006).
[14] S. F. Yelin, V. A. Sautenkov, M. M. Kash, G. R. Welch, and M. D. Lukin, Phys. Rev. A **68**, 063801 (2003).
[15] K. Yamamoto, K. Ichimura, and N. Gemma, Phys. Rev. A **58**, 2460 (1998).
[16] G. S. Agarwal, T. N. Dey, and S. Menon, Phys. Rev. A **64**, 053809 (2001).
[17] H. Li, V. A. Sautenkov, Y. V. Rostovtsev, G. R. Welch, P. R. Hemmer, and M. O. Scully, Phys. Rev. A **80**, 023820 (2009).
[18] D. V. Kosachiov and E. A. Korsunsky, Eur. Phys. J. D **11**, 457 (2000).
[19] K. V. Rajitha, T. N. Dey, S. Das, and P. K. Jha, Opt. Lett. **40**, 2229 (2015).
[20] S. Davuluri and Y. Rostovtsev, Phys. Rev. A **88**, 053847 (2013).
[21] L. Li and G. X. Huang, Eur. Phys. J. D **58**, 339 (2010).
[22] A. Eilam, A. D. Wilson-Gordon, and H. Friedmann, Opt. Lett. **34**, 1834 (2009).
[23] F. Renzoni, S. Cartaleva, G. Alzetta, and E. A. Arimondo, Phys. Rev. A **63**, 065401 (2001).
[24] A. Mair, J. Hager, D. F. Phillips, R. L. Walsworth, and M. D. Lukin, Phys. Rev. A **65**, 031802 (2002).
[25] G. S. Agarwal, T. N. Dey, and D. J. Gauthier, Phys. Rev. A **74**, 043805 (2006).
[26] X. Fernandez-Gonzalvo, Y. H. Chen, C. Yin, S. Rogge, and J. J. Longdell, Phys. Rev. A **92**, 062313 (2015).
[27] C. Champenois, G. Morigi, and J. Eschner, Phys. Rev. A **74**, 053404 (2006).
[28] A. M. Weiner, Rev. Sci. Instrum. **71**, 1929 (2000).
[29] R. Grobe, F. T. Hioe, and J. H. Eberly, Phys. Rev. Lett. **73**, 3183 (1994).
[30] T. N. Dey and G. S. Agarwal, Phys. Rev. A **67**, 033813 (2003).